

Trends in solar radiation due to clouds and aerosols, southern India, 1952–1997

Trent W. Biggs,^{a*} Christopher A. Scott,^b Balaji Rajagopalan^c and Hugh N. Turrall^d

^a *International Water Management Institute, Hyderabad, India 502324 Currently INTERA Incorporated, Niwot, CO, and Department of Civil, Environmental and Architectural Engineering, University of Colorado, Boulder.*

^b *International Water Management Institute, Hyderabad, India, currently Department of Geography and Regional Development, University of Arizona, Tucson, AZ 85721*

^c *Department of Civil, Environmental, and Architectural Engineering, University of Colorado, Boulder, CO, 80309*

^d *International Water Management Institute, Colombo, Sri Lanka*

Abstract:

Decadal trends in cloudiness are shown to affect incoming solar radiation (SW_{SFC}) in the Krishna River basin (13–20°N, 72–82°E), southern India, from 1952 to 1997. Annual average cloudiness at 14 meteorological stations across the basin decreased by 0.09% of the sky per year over 1952–1997. The decreased cloudiness partly balanced the effects of aerosols on incoming solar radiation (SW_{SFC}), resulting in a small net increase in SW_{SFC} in monsoon months (0.1–2.9 W m⁻² per decade). During the non-monsoon, aerosol forcing dominated over trends in cloud forcing, resulting in a net decrease in SW_{SFC} (–2.8 to –5.5 W m⁻² per decade). Monthly satellite measurements from the International Satellite Cloud Climatology Project (ISCCP) covering 1983–1995 were used to screen the visual cloudiness measurements at 26 meteorological stations, which reduced the data set to 14 stations and extended the cloudiness record back to 1952. SW_{SFC} measurements were available at only two stations, so the SW_{SFC} record was extended in time and to the other stations using a combination of the Angstrom and Hargreaves-Supit equations. The Hargreaves-Supit estimates of SW_{SFC} were then corrected for trends in aerosols using the literature values of aerosol forcing over India. Monthly values and trends in satellite measurements of SW_{SFC} from National Aeronautics and Space Administration's (NASA's) surface radiation budget (SRB) matched the aerosol-corrected Hargreaves-Supit estimates over 1984–1994 (RMSE = 11.9 W m⁻², 5.2%). We conclude that meteorological station measurements of cloudiness, quality checked with satellite imagery and calibrated to local measurements of incoming radiation, provide an opportunity to extend radiation measurements in space and time. Reports of decreased cloudiness in other parts of continental Asia suggest that the cloud-aerosol trade-off observed in the Krishna basin may be widespread, particularly during the rainy seasons when changes in clouds have large effects on incoming radiation compared with aerosol forcing. Copyright © 2007 Royal Meteorological Society

KEY WORDS radiation; climate change; global dimming; aerosols; remote sensing

Received 16 September 2006; Accepted 30 November 2006

INTRODUCTION

The flux of shortwave radiation at the ground surface (SW_{SFC}) drives many ecological and hydrological processes (Arora, 2002; Milly and Dunne, 2002). SW_{SFC} has decreased in many regions of the Earth because of increased aerosols from anthropogenic pollution, a process often referred to as 'global dimming' (Stanhill and Cohen, 2001; Liepert, 2002; Roderick and Farquhar, 2002). South Asia has particularly high aerosol concentrations, which may affect SW_{SFC} at regional scales (Pandithurai *et al.*, 2004; Liu *et al.*, 2005). Satellite measurements and ground-based pyranometers suggest that

SW_{SFC} decreased by up to 10% over parts of central India during the non-monsoon season (January–April) because of anthropogenic aerosols, which could have long-term effects on climate and rainfall over the sub-continent (Ramanathan *et al.*, 2001b; Ramanathan *et al.*, 2005).

In addition to forcing by anthropogenic aerosols, trends in cloudiness may also impact SW_{SFC} . Satellite data suggest that cloudiness over the tropics decreased over 1979–2001, leading to a decrease in shortwave radiation reflected off the top of the atmosphere (Wielicki *et al.*, 2002). Ground-based observations in parts of China (Kaiser, 2000) and continental Asia (Hahn and Warren, 2002; Warren *et al.*, submitted) also recorded regional decreases in cloud cover, which may have been caused by suppression of cloud formation by aerosols (Ackerman *et al.*, 2000), changes in atmospheric circulation (Chen *et al.*, 2002), changes in precipitation efficiency (Clement and Soden, 2005), or natural decadal variability (Cess and

* Correspondence to: Trent W. Biggs, International Water Management Institute, Hyderabad, India 502324 Currently INTERA Incorporated, Niwot, CO, and Department of Civil, Environmental and Architectural Engineering, University of Colorado, Boulder, USA.
E-mail: trentbren@yahoo.com

Udelhofen, 2003). Decreases in cloud cover over Asia might be expected to counteract the dimming effects of aerosols by increasing atmospheric transmissivity.

Detection of long-term trends in cloud and aerosol forcing of SW_{SFC} is complicated by the lack of historical data. SW_{SFC} measurements by pyranometers at the ground surface are often available for only a few sites and for a limited number of years, particularly in developing countries. The spatial density of pyranometer measurements is sufficient for global and regional analyses, but a higher density of measurements is required for water resources analysis in river basins. Satellite measurements from NASA's Surface Radiation Budget (Gupta *et al.*, 1999) cover a limited number of years (1984–1994), and longer time series are necessary to capture accurate means and trends in SW_{SFC} .

Where SW_{SFC} is not available from pyranometer or satellite measurements, it may be estimated using sunshine hours or cloudiness and temperature data (Allen *et al.*, 1996; Supit and van Kappel, 1998), but the cloudiness data need to be checked against independent measurements because of observer differences and changes in methodology (Karl and Steurer, 1990). Visual estimates of cloudiness also do not contain quantitative information on cloud radiative properties, so estimates of radiation derived from them must be checked against both ground-based and satellite measurements of radiation (Norris, 2000). Satellite measurements are also subject to some uncertainty due to viewing angle (Campbell, 2004) and the choice of threshold reflectance that defines a cloud (Norris, 2000). Changes in viewing angle can account for some of the decreasing trends in cloudiness observed over the period of satellite measurements (Campbell, 2004). Owing to the limitations and potential errors of both ground-based and satellite measurements of cloudiness and radiation, inter-comparison of the two can increase confidence in spatial and temporal trends recorded by each method.

This paper documents temporal trends in cloudiness and incoming shortwave radiation at the ground surface (SW_{SFC}) in the Krishna basin, southern India (258, 912 km²), over the period 1952–1997. Long-term, ground-based measurements of SW_{SFC} were available for only two of the 27 stations, so the SW_{SFC} record was extended using a combination of (1) the Angstrom equation calibrated to the two stations with pyranometer measurements, which predicted SW_{SFC} at seven stations with sunshine hours data, and (2) the Hargreaves equation as modified by Supit and Van Kappel (1998), which predicted SW_{SFC} from diurnal temperature range and cloudiness at the other stations without pyranometers or sunshine data. Trends in aerosol forcing, which were not accounted for by the Hargreaves-Supit equation, were derived from values of aerosol forcing measured by others over India (Ramanathan *et al.*, 2005) and incorporated as a linear trend to arrive at an estimate of SW_{SFC} corrected for trends in aerosol forcing. The SW_{SFC} calculated from the Hargreaves-aerosol equations were then compared with the satellite measurements

of SW_{SFC} to confirm that monthly patterns and trends were captured by both data sets. The cloudiness (26 stations) and SW_{SFC} data (two stations) were first checked against satellite observations from NASA's Solar Radiation Budget (Gupta *et al.*, 1999; Stackhouse *et al.*, 2001), and recommendations were made about which data to use for regional hydrologic and water resources modeling. The main questions included the following. (1) How do estimates of incoming radiation and cloudiness made at meteorological stations compare with satellite-based estimates? (2) Were there temporal trends in cloudiness in the Krishna basin over 1952–1997? (3) How did the trends in SW_{SFC} from changes in cloud forcing compare with trends in aerosol forcing, and what was the net trend in SW_{SFC} ? This paper contributes to a wider study on the interactions between climate, hydrology, and land use in the Krishna basin, and illustrates how widely available data sets from both satellites and meteorological stations can be used in studies of basin-scale radiation.

METHODS

Meteorological and satellite data sources

Data from 27 meteorological stations were available in and near the Krishna basin (Figure 1). A total of 26 stations were maintained by the Indian Meteorological Department (IMD), and one was maintained by the International Crops Research Institute for the semiarid tropics (ICRISAT), in the city Patancheru. Four stations had SW_{SFC} measurements for some years; the Pune and Patancheru stations had the longest and most complete records (Table AI). SW_{SFC} at Patancheru was measured with a LI200X Silicon pyranometer calibrated to 400–1100 nm, with a mean accuracy of 3–5%. Mean monthly sunshine hours, defined as the number of hours of bright sunlight per day as measured by a sunshine recorder, were available for ten stations starting in the 1970s, but simultaneous cloudiness and sunshine data were available at only seven stations. Monthly visual cloudiness estimates and temperature data were available for 26 stations in most years from the mid-1940s to 1997. Visual cloudiness estimates were made at 8:30 A.M. and 5:30 P.M. Indian Standard Time, and the average of the two was taken for the trend analysis and extension of the SW_{SFC} record.

Cloudiness and incoming shortwave radiation (SW_{SFC}) at 1 degree resolution from NASA's Surface Radiation Budget (SRB) Release 2 were downloaded from the Langley Atmospheric Sciences Data Center (http://eosweb.larc.nasa.gov/PRODOCS/srb/table_srb.html, access date 25 May 2006). Cloudiness was available from July 1983 to October 1995, and SW_{SFC} from March 1984 to September 1995. SW_{SFC} from the SRB has a mean bias of 0.9 W m⁻² and a mean error of ± 22 W m⁻² (http://eosweb.larc.nasa.gov/PRODOCS/srb/readme/readme_srb_rel2_sw_monthly.txt, access date 25 May 2006). The SRB monthly values were originally based

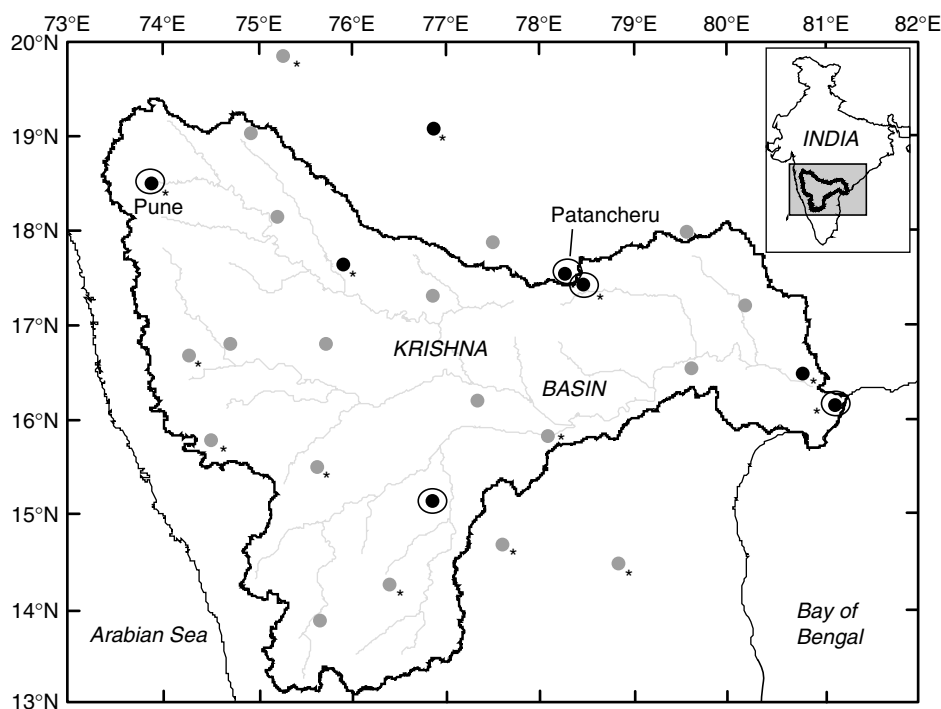


Figure 1. Location map of the Krishna basin and meteorological stations, coded by data availability. Grey dots indicate stations with cloudiness and temperature data; black dots indicate stations with cloudiness, temperature, and sunshine hours, and black dots with clear circles around them indicate stations with incoming solar radiation data measured with a pyranometer. * indicate the 14 quality-controlled stations.

on 3-hourly satellite measurements, then averaged to daily and monthly values. SW_{SFC} from the SRB was based on the Pinker–Laszlo algorithm (Pinker and Laszlo, 1992).

Monthly means and anomalies in SW_{SFC} were compared with the pyranometer measurements at the Pune and Patancheru stations. The Pune IMD station was located at 73.85° longitude on the Deccan Plateau, but we used the SRB cell at 74° longitude for comparison with the satellite data; the cell at 74° longitude covered a part of the Deccan Plateau and better represented the landscape and climate conditions at Pune than the cell at 73° , which was dominated by the Western Ghats.

The visual cloudiness observations from the meteorological stations were screened on the basis of completeness of record and consistency with the ISCCP data. Inclusion in the time series analysis required (1) data in all months for at least 90% of the years from 1952 to 1997 and (2) a Pearson correlation coefficient of at least 0.85 between the IMD and ISCCP cloudiness.

Angstrom and Hargreaves equations with correction for aerosols

A combination of the Angstrom equation, modified Hargreaves equation, and trends in aerosols from Ramanathan *et al.* (2005) was used to estimate SW_{SFC} for stations lacking data on incoming radiation or sunshine hours. Angstrom–Prescott proposed a relation between incoming radiation and sunshine hours, hereafter called the *Angstrom equation*, as cited in Supit and van

Kappel (1998):

$$\frac{SW_{SFC}}{SW_{TOA}} = A_a + B_a \frac{n}{N} \quad (1)$$

where SW_{SFC} is the incoming shortwave solar radiation flux measured at the ground surface ($W m^{-2}$), SW_{TOA} is the incoming shortwave radiation flux at the top of the atmosphere, A_a and B_a are coefficients, n is the hours of bright sunshine as measured by a Campbell–Stokes sunshine recorder, and N is the maximum possible hours of bright sunshine given the latitude and Julian day. N and SW_{TOA} were calculated from the latitude and Julian day (Allen, *et al.* 1996). The value of n/N is one on cloudless days, so the clear-sky transmissivity is $A_a + B_a$.

For time periods and stations where sunshine hours (n) were not available, the Hargreaves method as modified by Supit and Van Kappel (1998) was used to estimate SW_{SFC} (hereafter called *Hargreaves–Supit radiation*, SW_{Har}) following Supit and van Kappel (1998):

$$\frac{SW_{Har}}{SW_{TOA}} = A_s \sqrt{T_{max} - T_{min}} + B_s \sqrt{1 - CC/8} + \frac{C_s}{R_{e xo}} \quad (2)$$

where T_{max} and T_{min} are the monthly average maximum and minimum temperatures in $^\circ C$, A_s , B_s , and C_s are coefficients, and CC is visual cloud cover in okta (0–8), which is converted to sky fraction by dividing by 8. The Angstrom A_a and B_a values calibrated to the Patancheru and Pune stations were used to calculate

SW_{SFC}/SW_{TOA} for the seven stations with both sunshine hours and cloudiness data, which in turn determined the values of A_s , B_s , and C_s in the Hargreaves-Supit method through multiple linear regression. The mean values of A_s , B_s , and C_s were used to calculate incoming solar radiation for the remaining stations using Equation (2).

The Hargreaves-Supit relation (Equation 2) does not explicitly consider the effect of changes in the physical or optical properties of clouds on incoming radiation (Haurwitz, 1946; Kasten and Czeplak, 1980; Rossow and Lacis, 1990). Variability in cloud properties, including over small spatial scales (Rossow, 1989), may preclude the use of a simple relationship between visual cloud cover and incoming solar radiation as assumed in the Hargreaves relation. A full radiative transfer model (Chou and Zhao, 1997) or separate transmissivities by cloud type (Kasten and Czeplak, 1980) could account for cloud physical properties, but the IMD historical data used here cannot reliably predict those properties. The purpose of the present investigation is to test the utility of a simple relationship (Equation 2) appropriate for a given data set in a single river basin, and to use that relationship to leverage historical cloudiness data that do not include detailed cloud property measurements.

The Angstrom and Hargreaves-Supit relations implicitly included the long-term mean effect of aerosols on atmospheric transmissivity. For example, clear-sky transmissivity for the Angstrom equation was 0.69–0.76 at the IMD stations in the Krishna basin. The equations did not, however, quantify the changes in aerosol forcing with time except through a change in their parameter values. Since we used constant Angstrom and Hargreaves-Supit parameters for all the years, trends in the Hargreaves-Supit radiation caused by changes in cloudiness or diurnal temperature range had to be corrected for trends in anthropogenic aerosol forcing. Measurements of aerosol forcing include natural aerosols such as mineral dust, natural fires, and marine aerosols (Bellouin *et al.*, 2005); the anthropogenic contribution to aerosol forcing was estimated to be 80% of the total aerosol forcing over South Asia (Ramanathan *et al.*, 2001a). The trend in anthropogenic aerosol forcing over 1945–1995 is calculated as

$$\beta_{aer} = 0.8F_{aer}/50 \quad (3)$$

where F_{aer} is total aerosol forcing in $W\ m^{-2}$ measured over 1995–1999 by Ramanathan *et al.* (2005), 0.8 is the fraction of aerosol forcing estimated to be from anthropogenic sources (Ramanathan *et al.*, 2005), and 50 is the number of years between the time of minimal anthropogenic aerosol forcing (1945) and the observed anthropogenic aerosol forcing in 1995–1999. The trends in aerosol forcing calculated from Equation (3) agreed with the observed trends in aerosol forcing over India (Ramanathan *et al.*, 2005), suggesting that the approximation of zero anthropogenic aerosol forcing in 1945 gave a good approximation of the long-term trend.

The monthly or annual average incoming shortwave radiation may then be calculated from Equations (2) and (3) as

$$SW_{SFC} = SW_{Har} + \beta_{aer}(y - 1945) \quad (4)$$

where y is the year. Equation (4) will hereafter be called the *Hargreaves-aerosol equation*. The trends in SW_{SFC} are then separable into the trend due to aerosol forcing and the trend due to changes in cloudiness:

$$\beta_{net} = \beta_{Har} + \beta_{aer} \quad (5)$$

where β_{net} is the net trend in incoming radiation in $W\ m^{-2}\ y^{-1}$ for a given month, and β_{Har} is the linear trend in Hargreaves-Supit radiation for the month.

The aerosol model used to calculate F_{aer} by Ramanathan *et al.* (2005) included both the direct effects of aerosols on scattering and their indirect effects on clouds and cloud optical thickness. Some of the indirect effects, such as enhanced or inhibited cloud formation, may have been recorded by visual observations, which could have caused double-counting of the cloud effect in Equations (4) and (5) if the aerosol model also simulated cloud cover changes. However, the model of Ramanathan *et al.* (2005) did not produce decreased cloud cover for South Asia, so the effects of cloud cover change on SW_{SFC} were not double-counted in Equations (4) and (5).

RESULTS

Spatial patterns in cloudiness, aerosols, and solar radiation from satellite data

Satellite-based measurements of cloudiness from the International Satellite Cloud Climatology Project (ISCCP) (Rossow and Schiffer, 1991; Rossow and Schiffer, 1999) and incoming solar radiation from the NASA Surface Radiation Budget (SRB) (Gupta *et al.*, 1999; Stackhouse, Jr, *et al.*, 2001) had marked seasonal patterns associated with the monsoon (Figure 2). The critical months were May and June when the onset of the southwest monsoon increased cloudiness and decreased SW_{SFC} . Cloudiness was slightly higher in the Western Ghats during the monsoon and in the Krishna Delta during the non-monsoon compared with the basin average. The dry central basin had lower cloud cover than the Western Ghats or Krishna Delta in the pre-monsoon months (January–May). Average annual cloudiness decreased gradually from the Bay of Bengal to the Western Ghats, and increased from north to south (Figure 3(a)).

The Western Ghats occupy a relatively narrow strip along the west coast and may have higher cloudiness than the average of the 1×1 degree cells, a pattern that could be quantified using higher resolution data from the ISCCP. The rest of the basin is a flat plateau, so spatial variation of annual cloudiness within each 1×1 degree cell should be minimal. The low cloudiness off the west coast of India and decrease in cloudiness

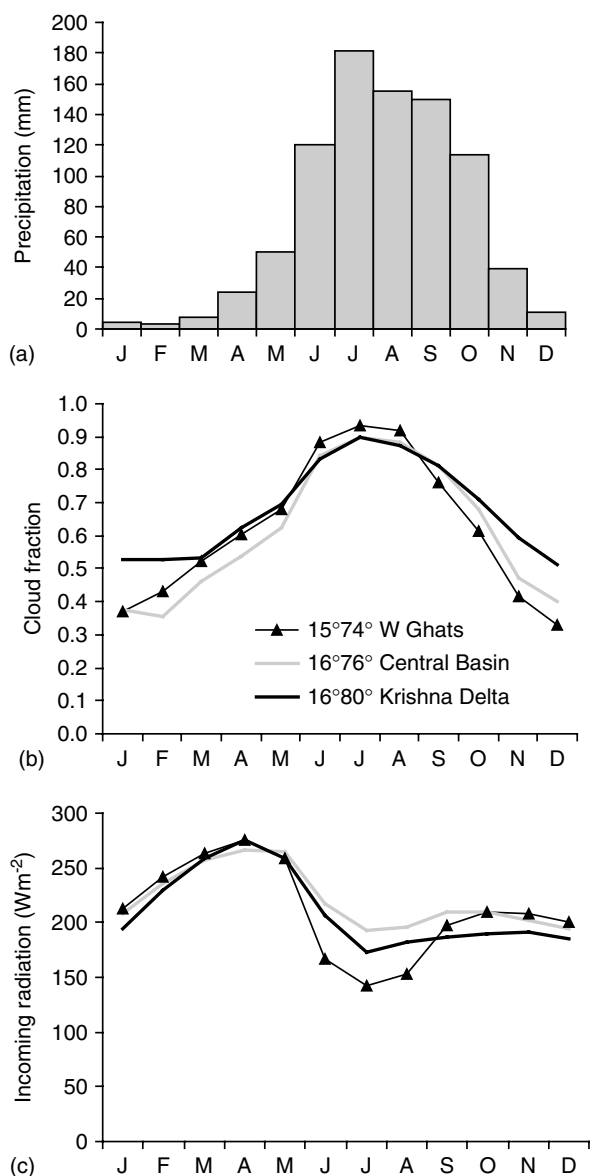


Figure 2. Monthly averages of (a) precipitation for the Krishna basin, and (b) cloudiness and (c) incoming radiation for the three regions of the basin. Precipitation data is from the Indian Institute of Tropical Meteorology.

from north to south (Figure 3(a)) matched data from the Extended Edited Cloud Reports Archive (Hahn and Warren, 2002).

Monthly incoming shortwave radiation at the ground surface (SW_{SFC}) measured by the SRB was uniform over the basin during the pre-monsoon months. SW_{SFC} was lower in the Western Ghats compared with the rest of the basin during the monsoon (Figure 2), and annual SW_{SFC} was lowest in the Western Ghats and the delta (Figure 3(b)).

Quality control of visual cloudiness data by comparison with satellite measurements

Mean monthly radiation from the SRB averaged 2% higher and 4% lower than the pyranometer measurements at Patancheru and Pune, respectively (Figure 4(a)).

Monthly values from SRB and the pyranometers may correlate owing to seasonal effects, so the monthly errors (Figure 4(b)) and monthly anomalies (Figure 4(c–d)) are also presented to compare the two data sets. The monthly anomalies, calculated as the difference between the observed value and the mean over the period of record for each data set, had lower error at Patancheru ($11 W m^{-2}$) than at Pune ($15 W m^{-2}$).

Fourteen of the 26 IMD stations satisfied both the quality-control criteria for cloudiness: a correlation coefficient between IMD and ISCCP cloudiness greater than 0.85, and cloudiness data in all months for at least 90% of the years from 1952 to 1997 (Table AI, Figure A1). In contrast to the monthly measurements at a given station, annual average cloudiness over 1983–1995 from ISCCP and IMD did not correlate well for all stations together (Figure 5), though the correlation was better for the 14 quality-controlled stations. The ISCCP data showed consistent regional patterns and spatial coherence, with a gradual decrease in cloudiness from south to north (Figure 3). The IMD data showed higher spatial heterogeneity and no consistent regional trends. This suggests several alternative hypotheses. First, both ground and satellite measurements of cloudiness may be accurate, but at different scales. This is possible for a given month, especially around the Western Ghats where there are steep spatial gradients in precipitation and, presumably, cloudiness. However, this seems less likely for a long-term mean and for stations on the Deccan Plateau where spatial gradients in long-term mean cloudiness should be minimal or gradual. Also, ground-based observers sample an area of 60–100 km diameter, which is similar to an area of 60–100 km diameter (Rossow *et al.* 1993), the 106-km pixel size of the ISCCP (256-km for the original ISCCP resample). A scale effect also does not account for poor correlations at stations that are near other stations with good correlations with the ISCCP values. Second, the ISCCP data may measure different types of clouds than the IMD station observers. The ISCCP algorithm uses both visible and infrared radiation to classify 30-km pixels as cloudy or clear, then aggregates to a 2.5×2.5 degree grid (Rossow and Schiffer, 1991). Use of infrared radiation may result in a different threshold for cloud definition compared with visual observers. However, this also does not account for good correlations at some stations and poor correlations at other nearby stations. Third, the time of day of the measurements differs. The ISCCP cloudiness measurement is the average of 3-hour measurements during daylight hours, while the IMD data is the average of two daily observations. While this might explain the systematic differences at all stations (e.g. ISCCP cloudiness is higher than IMD cloudiness for all stations), it does not explain why some IMD stations have better correlations than others, especially for adjacent stations. Fourth, station operators make consistent estimates of cloudiness at a given station, but each observer estimates cloud cover differently from other observers. This is the most likely possibility, since visual measurements are semi-quantitative and based on observer interpretation

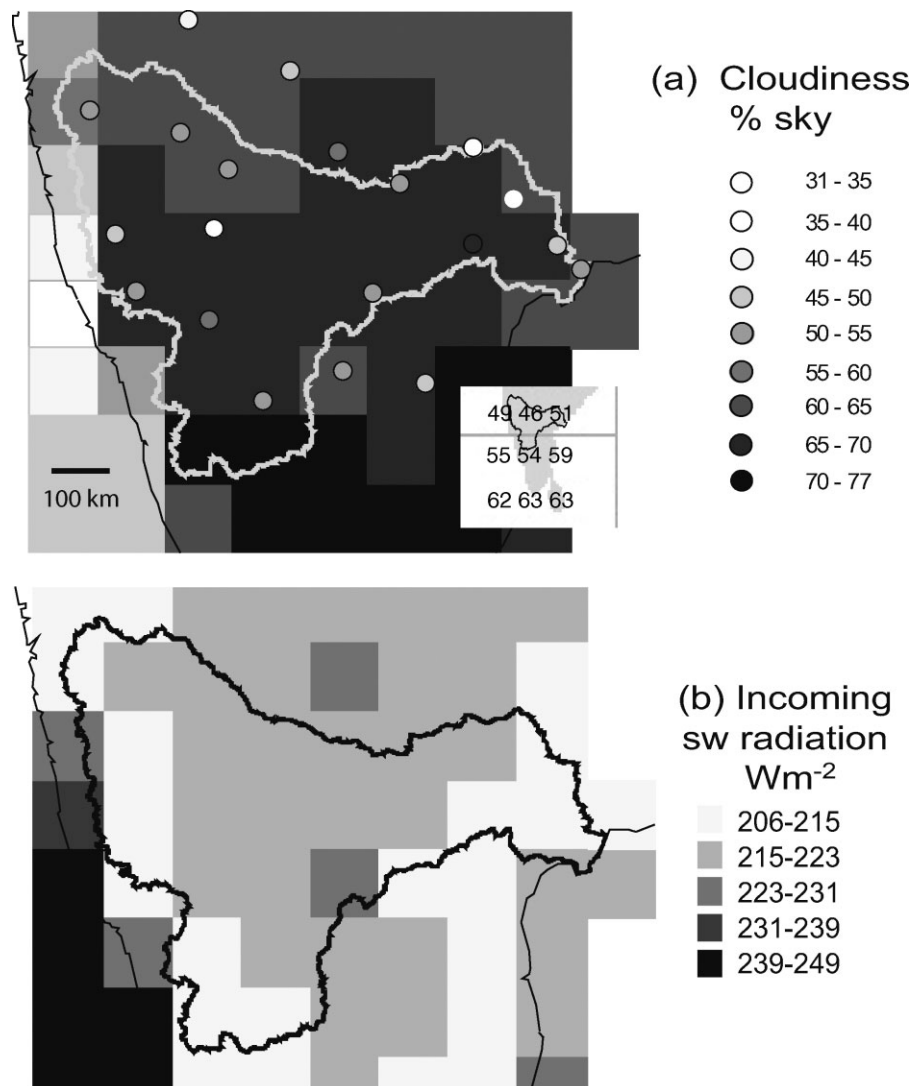


Figure 3. (a) Annual average cloudiness in 1986 from the ISCCP (grid) and IMD meteorological stations (circles). The grey-scale legend is the same for the two data sets. White areas of the grid that are not outlined have no data. The inset shows annual average cloudiness over southern India from the EECRA (Extended Edited Cloud Reports Archive) data set (Hahn and Warren, 2002; Warren *et al.*, submitted). (b) Annual average incoming shortwave radiation from the NASA Surface Radiation Budget (SRB) over 1983–1996, $W m^{-2}$.

(Karl and Steurer, 1990). Also, some stations with good correlations between the ISCCP and IMD values occur close to stations with poor correlations. This suggests that the mismatch between ISCCP and IMD stations is likely due to IMD observer differences rather than errors in the ISCCP algorithm. A more detailed comparison of the ISCCP and IMD cloud data, using daily observations and higher spatial resolution would help distinguish among these reasons for differences between the IMD and ISCCP data at individual stations.

In contrast to the low correlation between long-term average cloudiness estimated by ISCCP and IMD for the individual stations (Figure 5), basin-average cloudiness, monthly anomalies, and long-term trends over 1983–1995 agreed well between the two sources (Figure 6(a)). Monthly anomalies in the basin-average cloudiness from IMD matched the ISCCP measurements (RMSE 7.1% sky), though the means over the period were very different (IMD 48% sky *vs* ISCCP 62% sky),

possibly due to the use of infrared radiation for the ISCCP measurements, which may detect high and diffuse clouds not recorded by ground-based observers. Despite the difference in long-term mean cloudiness, both IMD and ISCCP gave similar negative trends in basin-average cloudiness over 1984–1995 (Figure 6(a)), though the trend from the IMD stations (2.4% per decade) was roughly half that of the ISCCP trend (5.2% per decade). The comparison suggests that the basin-average cloudiness from IMD produced similar monthly patterns and long-term trends as the ISCCP, so the IMD data can be used to document long-term trends.

Angstrom and hargreaves coefficients

The Angstrom coefficients A_a and B_a calibrated to monthly radiation and sunshine hours data at four stations compared well with the Angstrom parameters measured in other semiarid and arid regions (Table I). Two of the stations, Machilipatnam and Hyderabad, had relatively

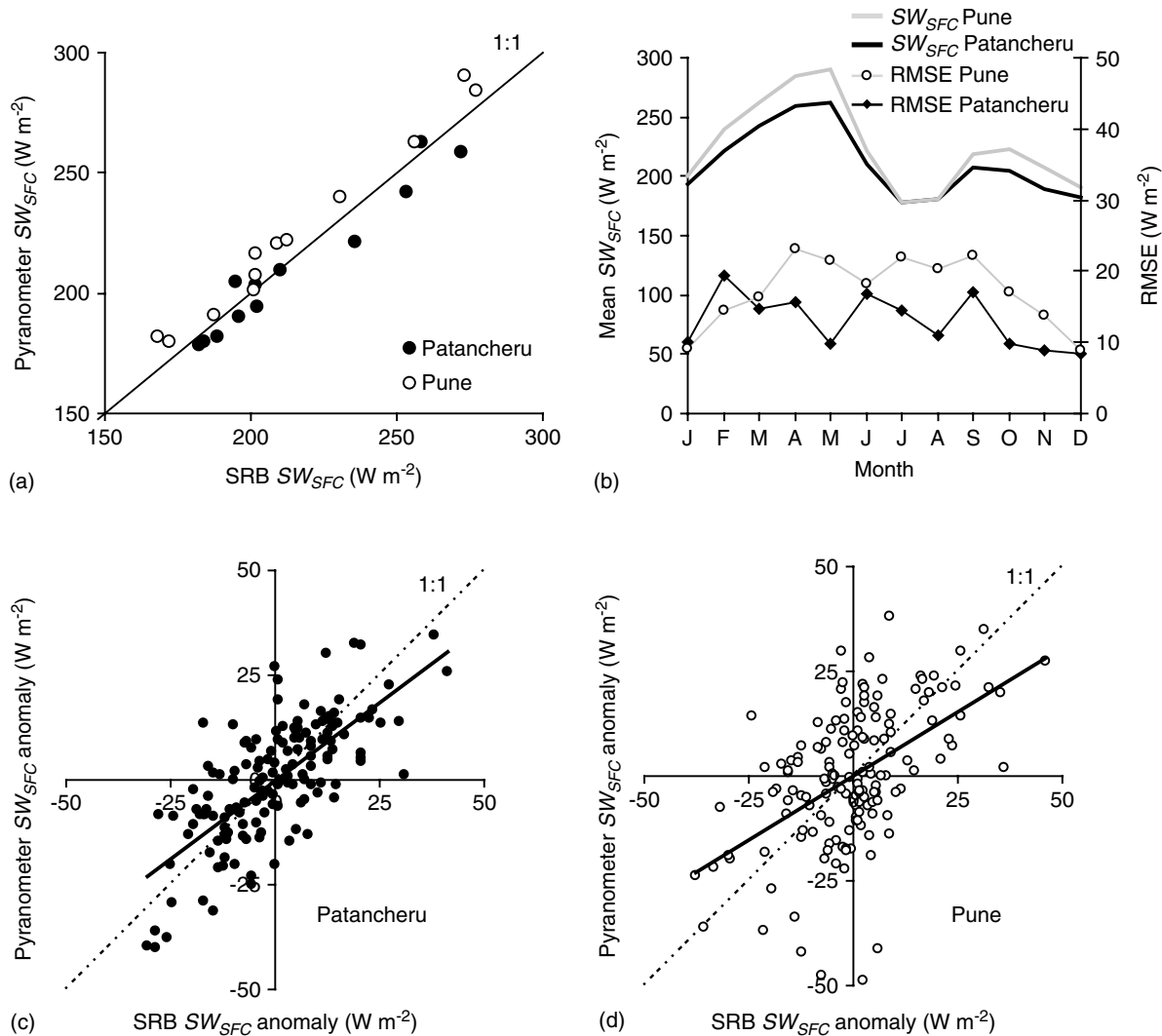


Figure 4. (a) Correlation between monthly average SW_{SFC} from the Surface Radiation Budget (SRB) and the pyranometer measurements over 1983–1995. (b) Monthly time series of average SW_{SFC} from the SRB, and the RMSE between the SRB and pyranometer measurements. (c–d) Monthly anomalies of SW_{SFC} from the SRB and pyranometer measurements at Patancheru and Pune.

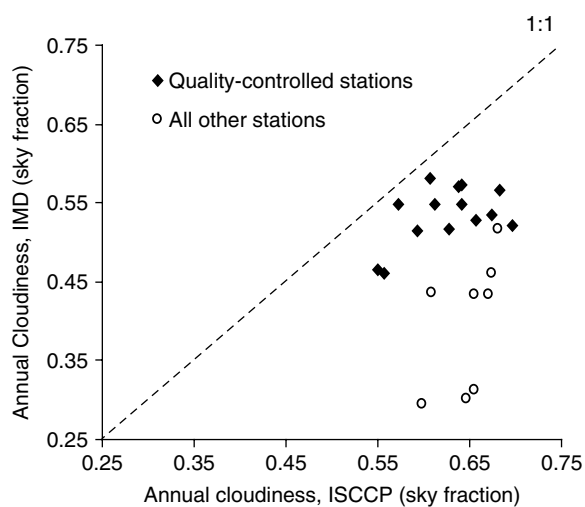


Figure 5. Annual average cloudiness measured by satellites (ISCCP) and the meteorological stations (IMD), separated into the 14 quality-controlled meteorological stations (black circles) and all other stations (white circles).

short records and poor fits with low R^2 values (Table I, Figure A2). The average of the Angstrom parameters at Patancheru and Pune were used to predict SW_{SFC} at stations with sunshine hours data. When using the average, it was assumed that spatial patterns in the Angstrom coefficients were minimal or due to local influences. The Angstrom parameters did not change from the first half to the last half of the record for either station (Figure A2).

The Angstrom parameters from Patancheru and Pune were used to calculate SW_{SFC}/SW_{TOA} for the five stations with sunshine hours but no radiation data. The SW_{SFC}/SW_{TOA} at all seven stations were then used to calibrate the Hargreaves coefficients for each station through multiple linear regression on Equation (2) (Figure A3). The values of A_s and B_s fell within the range observed in other semiarid climates, though some values of B_s fell below and values of C_s fell above the values observed in other regions (Table I). The differences in the values of A_s , B_s , and C_s among the Krishna basin stations and other

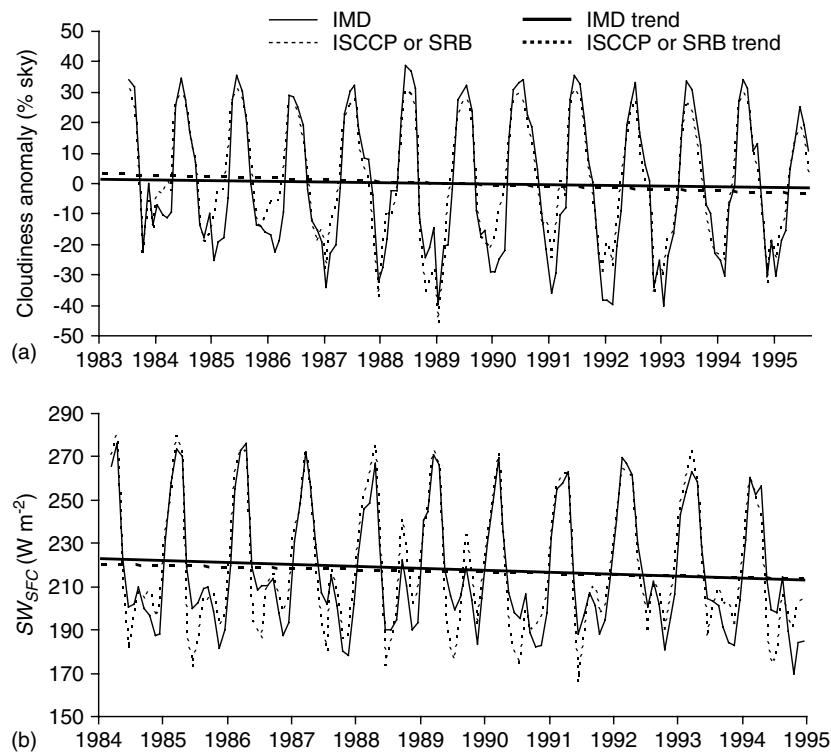


Figure 6. Monthly anomalies in basin-average (a) cloudiness and (b) incoming radiation (SW_{SFC}) from satellites (ISCCP for clouds or SRB for radiation) and the 14 quality-controlled IMD meteorological stations. SW_{SFC} at the IMD stations was calculated using the Hargreaves-Supit equation corrected for trends in aerosol forcing (Equation 4). The tick-marks indicate January of each year.

world stations may be partly due to collinearity between CC and $\sqrt{T_{max} - T_{min}}$, which can increase the variance of regression parameters (Montgomery and Peck, 1992).

Monthly SW_{SFC} averaged over the basin from the SRB matched SW_{SFC} from the Hargreaves-aerosol equation (Equation 4) (RMSE 11.9 W m^{-2} , Figure 6(b)), and SW_{SFC} both methods had negative trends over 1984–1994. The long-term mean SW_{SFC} was nearly the same between the two methods (217 W m^{-2} for SRB vs 218 W m^{-2} for IMD). Similar to the trends in cloudiness, the Hargreaves-aerosol equation gave a slightly smaller trend (-6.2 W m^{-2} per decade) than the SRB (-8.9 W m^{-2} per decade). The trends over 1984–1994 were larger than the long-term trends from the full 1952–1997 time series (see below) due to the influence of low SW_{SFC} in 1994 (Figure 6(b)). This shows the importance of considering a long time series for quantifying the trends. We conclude that basin-average cloudiness data from the IMD stations and SW_{SFC} estimated by Equation (4) may be used with confidence for establishing long-term trends over 1952–1997.

Trends over 1952–1997

Trends in (1) cloudiness from visual observations at the 14 quality-controlled stations, (2) SW_{SFC} measured by pyranometers at Pune and Patancheru, (3) SW_{HAR} , the incoming shortwave radiation estimated by the

Hargreaves-Supit equation, and (4) SW_{SFC} , the incoming shortwave radiation from the Hargreaves-Supit equation corrected for trends in aerosol forcing (Equation 4) were tested using linear regression with time as the independent variable. Parametric linear regression was used instead of the commonly used non-parametric Mann–Kendall test because the data were normally distributed, and the parametric test gives a more powerful test of trend.

Mean annual cloudiness at the 14 quality-controlled stations decreased by 0.09% of the sky per year, from 52% to 48% over 1952–1997 (Figure 7(a), $p < 0.05$). Changes in annual cloud cover over the basin were spatially variable; four of the 14 stations had statistically significant decreases in cloudiness and one had an increase (Pune, $p < 0.1$, Figure 8). Spatial heterogeneity in the trends in cloudiness could cause conflicting conclusions, depending on the data set used. The ensemble average used here showed trends that were obscured by inter-annual variability in individual station measurements. Decreasing annual cloudiness over 1952–1997 coincided with increased atmospheric pressure at the IMD stations ($p < 0.01$, Figure 7(b)). Five of the 27 stations had statistically significant decreases in precipitation in MAM, but there was no significant trend in annual rainfall over 1952–1997.

Basin-average annual SW_{HAR} , which changes with cloudiness, increased modestly by 6.5 W m^{-2} or 2% of the 1950s mean ($+0.13 \text{ W m}^{-2} \text{ y}^{-1}$) over 1952–1997 (Figure 7(d)). The positive trend in annual SW_{HAR} was

Table I. (a) Angstrom coefficients for semiarid locations and the Krishna basin. A_a and B_a are unitless. (b) Hargreaves coefficients for semiarid locations and the Krishna basin. A_s is in $^{\circ}\text{C}^{-1/2}$, B_s is unitless, C_s is in $\text{MJ m}^{-2} \text{ day}^{-1}$.

a. Angstrom coefficients	A_a	B_a	$A_a + B_a$	R^2	Reference ^a	
India (10 stations)	0.32	0.43	0.75	–	Martinez-Lozano <i>et al.</i> (1984)	
India (17 stations)	0.28	0.47	0.75	–	Martinez-Lozano <i>et al.</i> (1984)	
India (16 stations)	0.30	0.45	0.75	–	Martinez-Lozano <i>et al.</i> (1984)	
India (17 stations)	0.29	0.48	0.77	–	Martinez-Lozano <i>et al.</i> (1984)	
Jullundur, India	0.23	0.58	0.81	–	Martinez-Lozano <i>et al.</i> (1984)	
Madras, India	0.31	0.43	0.74	0.99	Martinez-Lozano <i>et al.</i> (1984)	
New Delhi, India	0.23	0.58	0.89	0.86	Martinez-Lozano <i>et al.</i> (1984)	
Middle East (23 stations)	0.27	0.49	0.76	–	Martinez-Lozano <i>et al.</i> (1984)	
East Africa (5 stations)	0.25	0.50	0.75	–	Martinez-Lozano <i>et al.</i> (1984)	
Valencia, Spain	0.26	0.44	0.70	–	Martinez-Lozano <i>et al.</i> (1984)	
Yemen	0.26	0.45	0.71	–	Martinez-Lozano <i>et al.</i> (1984)	
Giza, Egypt	0.25	0.47	0.72	–	Martinez-Lozano <i>et al.</i> (1984)	
Krishna basin						
ICRISAT station	0.26	0.44	0.69	0.92	This study	
Pune (43 063)	0.28	0.48	0.75	0.91	This study	
Hyderabad	0.26	0.50	0.76	0.52	This study	
Machilipatnam	0.24	0.46	0.70	0.68	This study	
Mean	0.26	0.46	0.72		This study	
Mean of ICRISAT, Pune	0.27	0.46	0.73		This study	
b. Modified Hargreaves	A_s	B_s	C_s	C_s/R_{exo}	R^2	
Murcia, Spain	0.12	0.26	–0.22	–	–	(Supit and van Kappel, 1998)
Mallorca, Spain	0.07	0.44	n.s	–	–	(Supit and van Kappel, 1998)
Central Turkey (Ankara)	0.05	0.40	0.0	–	–	(Micale and Genovese, 2004)
Raqqa, Syria	0.06	0.39	0.6	–	–	(Micale and Genovese, 2004)
Kharabo, Syria	0.03	0.36	2.5	–	–	(Micale and Genovese, 2004)
Krishna basin stations ^b						
43 063	0.062	0.25	4.3	0.18	0.75	This study
43 128	0.027	0.38	5.2	0.21	0.69	This study
43 181	0.049	0.36	3.5	0.14	0.57	This study
43 185	n.s	0.45	5.4	0.22	0.68	This study
43 017	0.059	0.39	2.4	0.10	0.71	This study
43 117	0.063	0.40	1.5	0.06	0.72	This study
43 205	0.069	0.19	5.6	0.23	0.63	This study
Average, Krishna stations	0.055	0.35	4.0	0.16	–	This study

^a All Angstrom references are as cited in Martinez-Lozano *et al.* 1984.

^b All Hargreaves parameters listed are significant to $p < 0.05$.

balanced by the negative trends due to aerosol forcing, and the net annual trend in SW_{SFC} (β_{net}) was negative (-1.3 W m^{-2} per decade, Figure 7(e)). The trend in SW_{SFC} from the Hargreaves-aerosol equation (Equation 4) was less than the trend in pyranometer measurements at Pune (2.2 W m^{-2} per decade) and less than the all-India average decrease in SW_{SFC} of $3.7\text{--}4.2 \text{ W m}^{-2}$ per decade (Ramanathan *et al.*, 2005). Basin-average SW_{Har} , which is sensitive to changes in cloud forcing, increased from April to September at a rate of 2.1 to 3.2 W m^{-2} per decade, depending on the month, except for June, which showed no increase (Figure 9). Like the trends in cloudiness, trends in SW_{Har} were spatially heterogeneous: annual average SW_{Har} increased at four of the 14 stations ($p < 0.1$) and decreased at one station (Pune, Figure 8(b)).

Decreases in SW_{SFC} due to anthropogenic aerosol forcing dominated over increases due to cloudiness

changes during the non-monsoon months, resulting in a negative net trend over 1952–1997 (Figure 9(a)). During the monsoon, aerosol forcing was small compared with trends due to cloudiness changes, resulting in a net positive trend in SW_{SFC} . Monthly trends in SW_{SFC} were similar for the pyranometer measurements and the Hargreaves-aerosol estimates (Figure 9(b), (c)). The more negative trend at Patancheru during the late monsoon (October) and post-monsoon (November–January) may have been due to the proximity of Patancheru to a large industrial area and the city of Hyderabad, or to changes in cloud optical properties not accounted for in the visual cloud observations. SW_{SFC} estimated with the Hargreaves-aerosol equation (Equation 4) compared well with pyranometer measurements and can be used with confidence to quantify long-term trends over the basin.

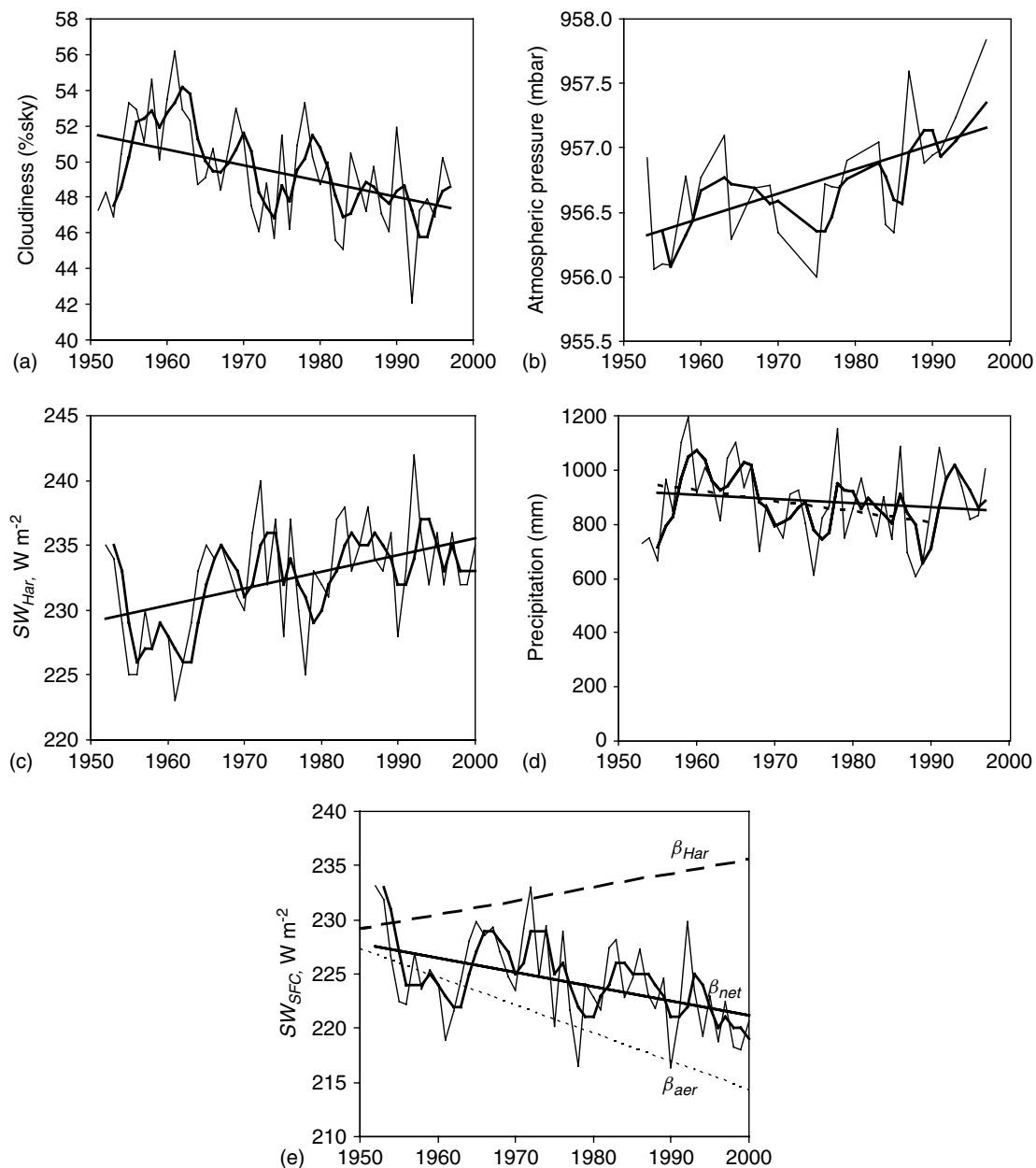


Figure 7. Temporal trends in basin-average meteorological parameters, including (a) annual cloudiness, (b) atmospheric pressure, (c) Hargreaves-Supit incoming solar radiation, (d) precipitation, and (e) incoming shortwave radiation (SW_{SFC}) for the 14 quality-controlled meteorological stations. (e) Includes the trend in Hargreaves-Supit radiation from (c) (β_{Har} , dashed line), the trend in aerosol forcing (β_{aer} , dotted line), and the net trend (β_{net} , solid line).

DISCUSSION AND CONCLUSION

The decrease in cloudiness observed in the Krishna basin has also been observed over the global tropics (Cess and Udelhofen, 2003; Wielicki *et al.*, 2002), parts of mainland China (Kaiser, 2000), and the larger south Asian region (Figure 8) (Warren *et al.*, submitted). The simultaneous increase in atmospheric pressure in the Krishna basin also occurred in parts of mainland China and is consistent with greater atmospheric stability and lower probability of cloud formation (Kaiser, 2000). Some parts of the trend in cloudiness from satellite imagery may be artifacts produced by the changes in viewing angle (Campbell, 2004). In the Krishna basin,

the ground observations and satellite data agree that cloudiness has decreased (Figure 6), which increased our confidence that the cloudiness trend was not a methodological artifact.

The trends in cloudiness may be caused by at least three processes: inhibition of cloud formation by aerosols (Ackerman *et al.*, 2000), changes in general circulation (Chen *et al.*, 2002), or changes in precipitation efficiencies (Clement and Soden, 2005). The interactions between aerosols and cloud formation complicate the complete separation of their effects on radiation, since aerosols may either enhance (Albrecht, 1989) or inhibit (Ackerman *et al.*, 2000) cloud formation. The model of Ramanathan *et al.* (2005) simulated the indirect effects of

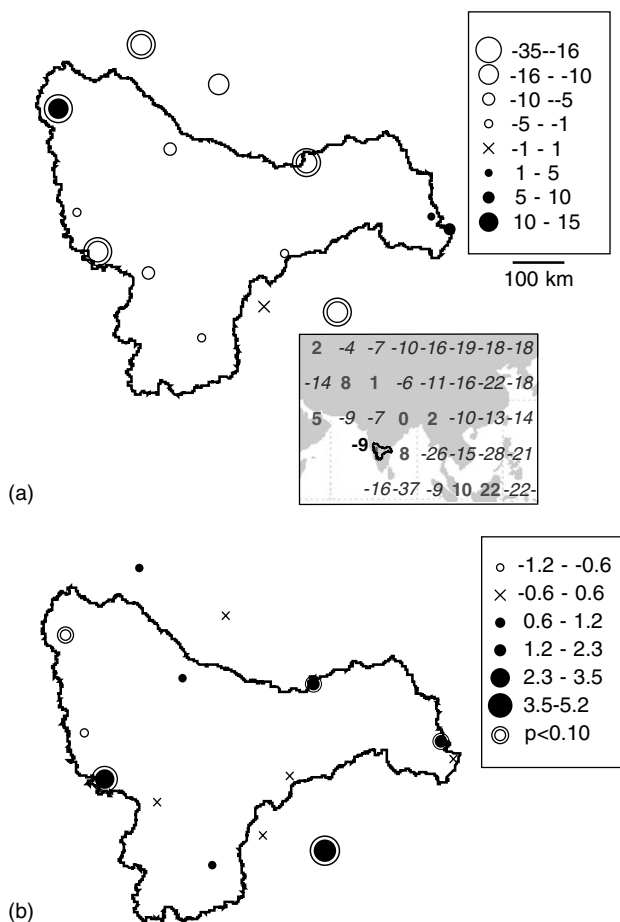


Figure 8. Map of trends in (a) annual cloudiness (0.1% sky per decade) and (b) incoming shortwave radiation (W m^{-2} per decade) for the 14 quality-controlled stations. A second ring indicates a statistically significant trend ($p < 0.1$). Inset in the lower right-hand corner of (a) shows the cloudiness trend values for continental Asia from the EECRA data set (Warren *et al.*, submitted, <http://www.atmos.washington.edu/CloudMap/>). The black -9 in the inset is the trend in mean cloudiness of the Krishna basin stations.

aerosols, including cloud inhibition, but found no change in cloud cover over India. This suggests that our use of the Hargreaves-Supit relation did not double-count the effects of cloud forcing, and that several processes may be contributing to the changes in cloudiness over the basin, in addition to aerosol inhibition of cloud formation.

Regardless of the mechanism causing the trends in cloudiness, the Krishna basin results showed that changes in radiation due to changes in cloud cover can dominate over aerosol forcing, especially during rainy periods when direct aerosol effects are small (Figure 9). The importance of cloud forcing during rainy periods and of aerosols during dry periods was also noted for the Amazon basin (Tarasova *et al.*, 2000). Decreases in incoming radiation have been inferred in many temperate and tropical regions (Stanhill and Cohen, 2001), and is likely due to anthropogenic aerosols (Roderick and Farquhar, 2002). The Krishna basin results show that decreases in cloud cover may compensate for aerosol forcing, resulting in

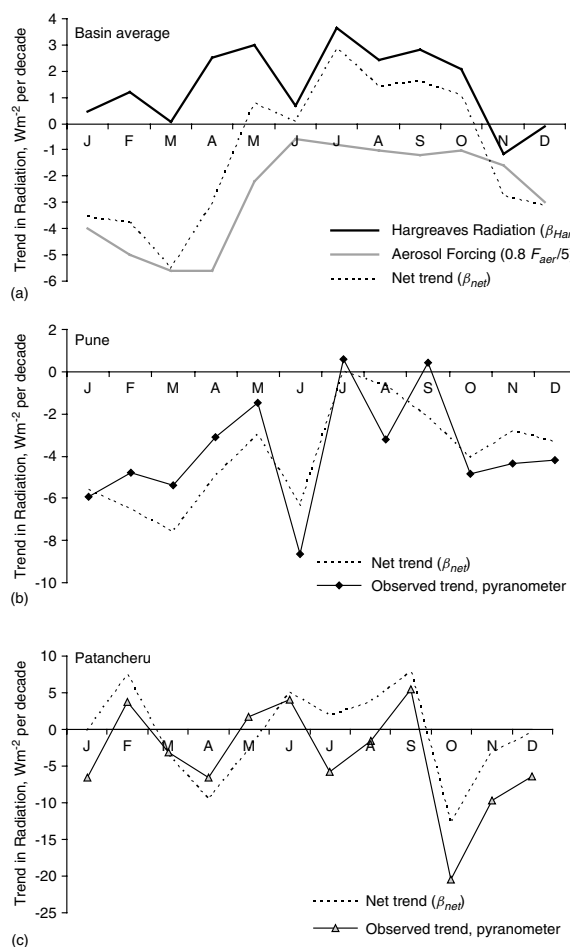


Figure 9. (a) Monthly trends in incoming shortwave radiation over the Krishna basin due to aerosol forcing (grey line, β_{aer}), Hargreaves-Supit radiation (black line, β_{Har}), and the net trend (dotted line, β_{net}) from Equation (5). (b–c) Net trends in incoming shortwave radiation (β_{net}) compared with observed trends at (b) Pune, 1957–1997 and (c) Patancheru, 1978–1997.

net increases in radiation in the rainy seasons. This phenomenon may be relatively widespread, given the recent observations of decreasing cloudiness over the tropics (Cess and Udelhofen, 2003) and continental Asia (Warren *et al.*, submitted). The Krishna basin results also show how the trends in basin-scale cloudiness and radiation can be documented and cross validated at high spatial resolution using a combination of measurements from satellites and meteorological stations.

ACKNOWLEDGEMENTS

This research was funded with a grant from the Australian Council for International Agricultural Research, and by donors to the International Water Management Institute. The ISCCP and SRB data were obtained from the NASA Langley Research Center Atmospheric Sciences Data Center. Many thanks to Frank Rijsberman for support.

APPENDIX

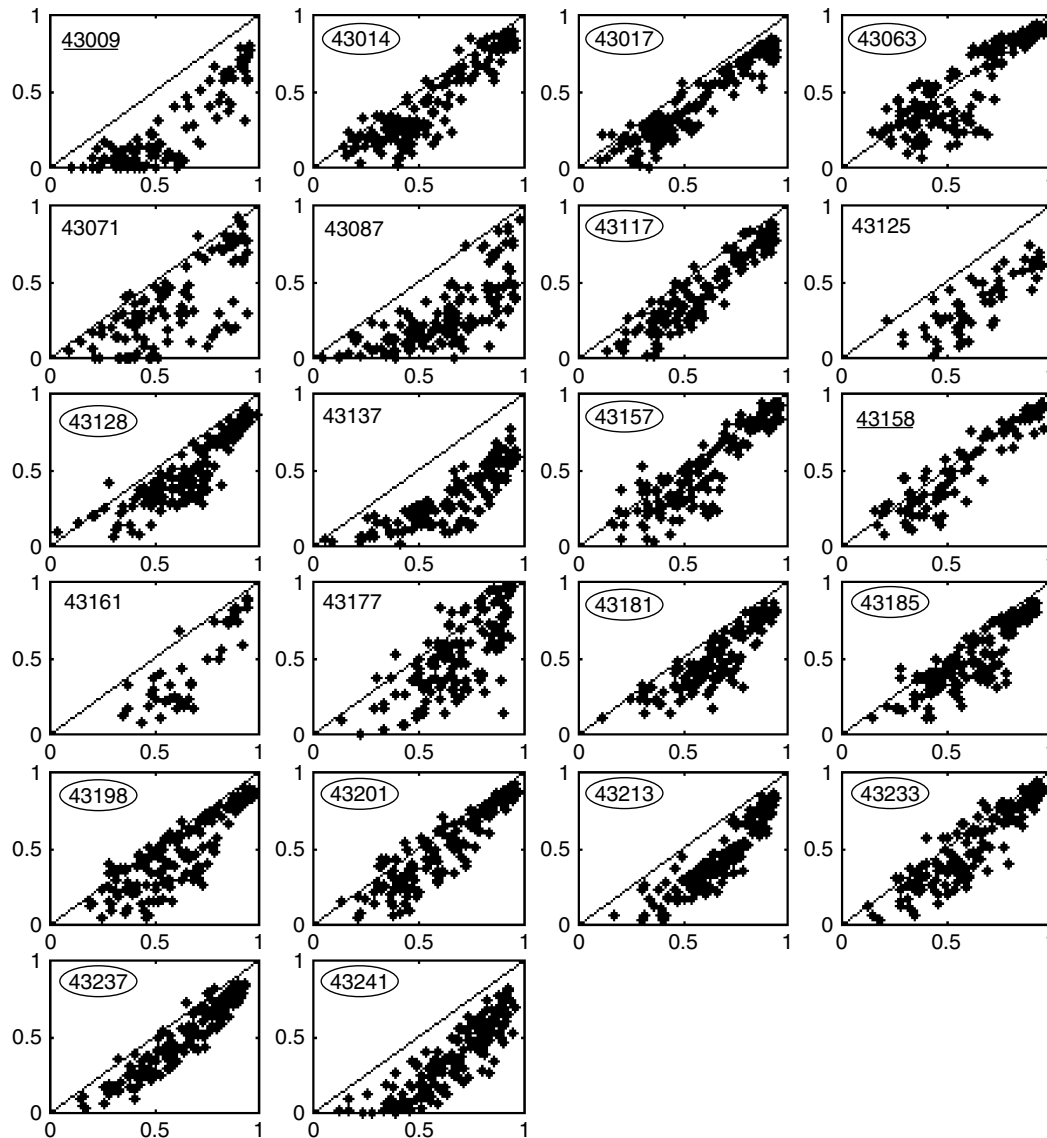


Figure A1. Monthly ISCCP cloudiness (x-axis) versus IMD station data (y-axis). Numbers in the upper left corner of each plot indicate the station code, circled codes indicate the 14 quality-controlled stations included in the analysis, and underlined codes indicate stations that had a correlation coefficient greater than 0.85 but had data for less than 90% of the months from 1952 to 1997. See Table AI for the metadata and correlation coefficients for each station. Four stations (43 205, 43 121, 43 169, 43 258) had insufficient data for the comparison, so data from 22 of the 26 stations with cloudiness data are shown.

REFERENCES

- Ackerman AS, Toon OB, Stevens DE, Heymsfield AJ, Ramanathan V, Welton EJ. 2000. Reduction of tropical cloudiness by soot. *Science* **288**: 1042–1047.
- Albrecht BA. 1989. Aerosols, cloud microphysics, and fractional cloudiness. *Science* **245**: 1227–1230.
- Allen RG. 2000. Using the FAO-56 dual crop coefficient method over an irrigated region as part of an evapotranspiration intercomparison study. *Journal of Hydrology* **229**: 27–41.
- Allen RG, Pereira LS, Raes D, Smith M. 1996. *Crop Evapotranspiration*. Food and Agriculture Organization: Rome.
- Arora VK. 2002. The use of the aridity index to assess climate change effect on annual runoff. *Journal of Hydrology* **265**: 164–177.
- Bellouin N, Boucher O, Haywood J, Shekar Reddy M. 2005. Global estimate of aerosol direct radiative forcing from satellite measurements. *Nature* **438**: 1138–1141 DOI: 10.1038/nature04348.
- Campbell GG. 2004. *View Angle Dependence of Cloudiness and the Trend in ISCCP Cloudiness*. Thirteenth Conference on Satellite Meteorology and Oceanography: Norfolk, VA.
- Cess RD, Udelhofen PM. 2003. Climate change during 1985–1999: cloud interactions determined from satellite measurements. *Geophysical Research Letters* **30**: (1):1019 DOI: 10.1029/2002GL016128.
- Chen J, Carlson BE, Del Genio AD. 2002. Evidence for strengthening of the tropical general circulation in the 1990s. *Science* **295**: 838–841.
- Chou M-D, Zhao W. 1997. Estimation and model validation of surface solar radiation and cloud radiative forcing using TOGA COARE measurements. *Journal of Climate* **10**: 610–620.
- Clement AC, Soden B. 2005. The sensitivity of the tropical-mean radiation budget. *Journal of Climate* **18**: 3189–3203.
- Gupta SK, Ritchey NA, Wilber AC, Whitlock CH, Gibson GG, Stackhouse PWJ. 1999. A climatology of surface radiation budget derived from satellite data. *Journal of Climate* **12**: 2691–2710.
- Hahn CJ, Warren SG. 2002. *Climatic Atlas of Clouds Over Land*. Oak Ridge National Laboratory: Oak Ridge, TN.
- Haurwitz B. 1946. Insolation in relation to cloud type. *Journal of Meteorology* **3**: 123–126.

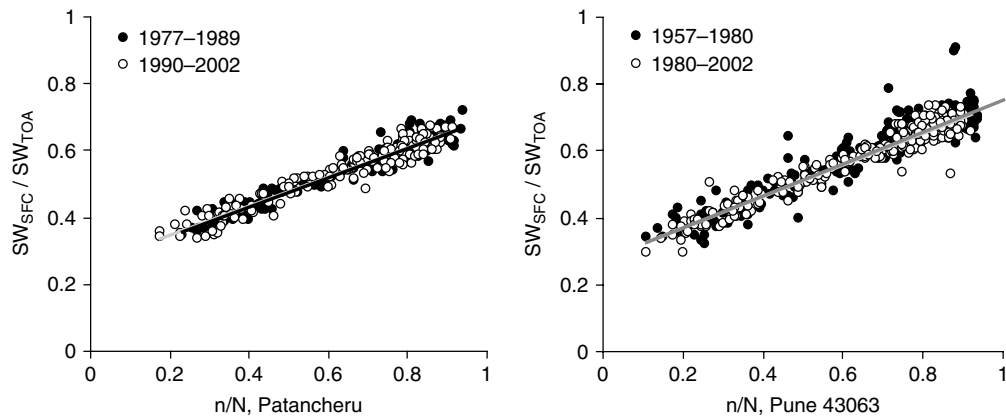


Figure A2. Angstrom relations between sunshine hours and incoming solar radiation for the Patancheru and Pune meteorological stations. The time series for each station was divided into early and recent, which varied for each station, depending on the period of available record. The light grey line is the regression or the early time series, and the dark grey line is for the recent time series. n is observed hours of bright sunshine, N is maximum possible hours of bright sunshine, SW_{SFC} is incoming shortwave solar radiation at the ground surface, SW_{TOA} is incoming radiation at the top of the atmosphere.

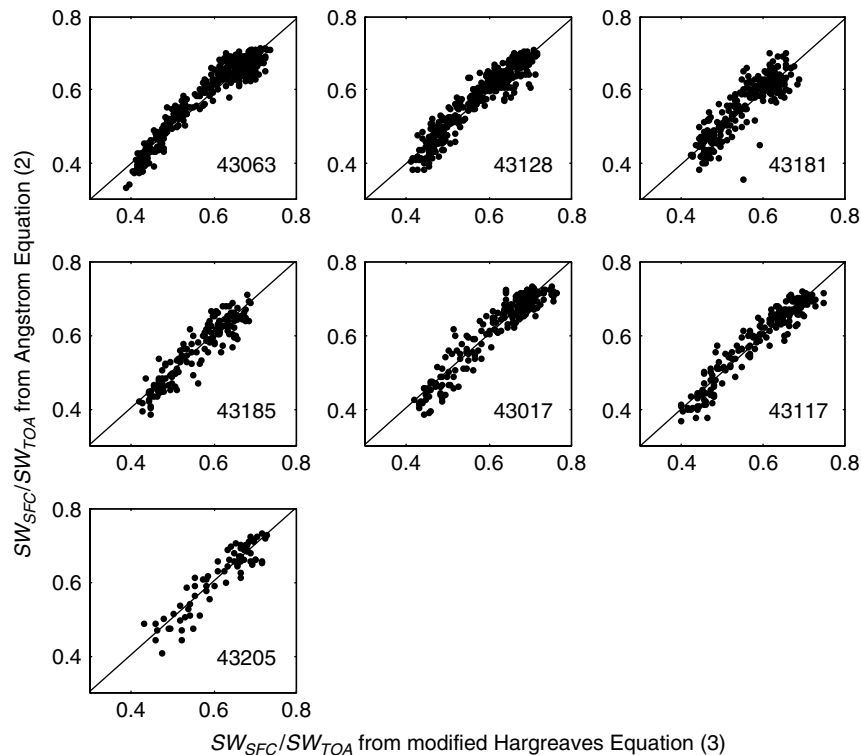


Figure A3. Comparison of Angstrom and Hargreaves-Supit equations predictions of SW_{SFC}/SW_{TOA} at seven meteorological stations in the Krishna basin.

Kaiser DP. 2000. Decreasing cloudiness over China: an updated analysis examining additional variables. *Geophysical Research Letters* **27**: 2193–2196.

Karl TR, Steurer PM. 1990. Increased cloudiness in the United States during the first half of the twentieth century: fact of fiction? *Geophysical Research Letters* **17**: 1925–1928.

Kasten F, Czeplak G. 1980. Solar and terrestrial radiation dependent on the cloud amount and type of cloud. *Solar Energy* **24**: 177–189.

Liepert BG. 2002. Observed reductions of surface solar radiation at sites in the United States and worldwide from 1961 to 1990. *Geophysical Research Letters* **29**: 61–61, CiteID 1421, DOI 10.1029/2002GL014910.

Liu H, Wonsick M, Pinker RT. 2005. *Aerosol Effects on the Surface Radiation Budget Over the Indian Monsoon Region*. American Geophysical Union Conference: San Francisco, CA.

Martinez-Lozano JA, Tena F, Onrubia JE, De la Rubia J. 1984. The historical evolution of the Angstrom formula and its modifications; review and bibliography. *Agricultural and Forest meteorology* **33**: 109–128.

Micale F, Genovese G. 2004. *Methodology of the MARS crop yield forecasting system; Meteorological data collection, processing and analysis*. Eur 21291 EN/1-4. European Commission Joint Research Center, http://agrifish.jrc.it/marsstat/crop_yield_forecasting/METAMP accessed October 2006.

Milly PCD, Dunne KA. 2002. Macroscale water fluxes 2. Water and energy supply control of their interannual variability. *Water Resources Research* **38**: 1206, DOI: 10.1029/2001WR000760.

Montgomery DC, Peck EA. 1992. *Introduction to Linear Regression Analysis*. John Wiley & sons, Ltd; New York.

Norris JR. 2000. What can cloud observations tell us about climate variability? *Space Science Reviews* **94**: 375–380.

Table A1. Metadata for the meteorological stations in and near the Krishna basin. N is the number of years of available record. * indicates the 14 quality-controlled stations that have both a complete record over 1952–1997 and a close match with satellite-based cloud cover estimates (Figure A1). ISCCP-IMD is the Pearson correlation coefficient between cloudiness derived from satellite imagery (ISCCP) and visual estimates at meteorological stations (IMD).

Station	Solar radiation		Sunshine hours		Cloudiness		r ISCCP-IMD	RMSE	f IMD 1952–97
	Years	N	Years	N	Years	N			
43 063 (Pune)*	57–02	46	57–02	46	53–02	49	0.85	0.15	0.98
Patancheru	77–03	27	75–03	29	–	–	–	–	–
43 128*	78–01	24	78–01	24	51–98	46	0.89	0.19	0.98
43 185*	85–01	17	85–01	17	47–98	46	0.87	0.16	0.94
43 205	74–84	11	74–97	24	49–85	27	–	–	–
43 009	93–01	7	97, 01	2	46–00	32	0.88	0.35	0.86
43 008	–	–	78–97	20	–	–	–	–	–
43 181*	–	–	69–98	30	49–98	46	0.87	0.19	0.97
43 017*	–	–	80–98	19	49–01	43	0.94	0.16	0.97
43 117*	–	–	77–97	19	48–00	50	0.93	0.17	0.96
43 014*	–	–	–	–	52–01	48	0.91	0.17	0.98
43 071	–	–	–	–	51–99	32	0.72	0.30	0.97
43 087	–	–	–	–	46–98	37	0.73	0.38	0.92
43 121	–	–	–	–	50–85	28	–	–	–
43 125	–	–	–	–	50–88	31	0.82	0.31	0.77
43 137	–	–	–	–	46–98	38	0.84	0.35	0.97
43 157*	–	–	–	–	51–01	48	0.90	0.15	0.99
43 158	–	–	–	–	40–01	34	0.93	0.11	0.74
43 161	–	–	–	–	49–88	33	0.86	0.28	0.75
43 169	–	–	–	–	49–86	27	–	–	–
43 177	–	–	–	–	48–98	51	0.72	0.24	0.93
43 198*	–	–	–	–	53–00	48	0.88	0.18	0.97
43 201*	–	–	–	–	49–00	52	0.91	0.15	0.97
43 213*	–	–	–	–	48–98	51	0.91	0.24	0.97
43 233*	–	–	–	–	48–00	53	0.91	0.14	0.93
43 237*	–	–	–	–	48–98	51	0.95	0.16	0.97
43 241*	–	–	–	–	48–98	51	0.87	0.31	0.97
43 258	–	–	–	–	51–80	30	–	–	–

Pandithurai G, Pinker RT, Takamura T, Devara PCS. 2004. Aerosol radiative forcing over a tropical urban site in India. *Geophysical Research Letters* **31**: L12107, Doi 10.1029/2004GL019702.

Pinker RT, Laszlo I. 1992. Modeling surface solar irradiance for satellite applications on a global scale. *Journal of Applied Meteorology* **31**: 194–211.

Ramanathan V, Curtzen PJ, Kiehl JT, Rosenfeld D. 2001b. Aerosols, climate, and the hydrological cycle. *Science* **294**: 2119–2124.

Ramanathan V, Chung K, Kim D, Bettge T, Buja L, Kiehl JT, Washington WM, Fu Q, Sikka DR, Wild M. 2005. Atmospheric brown clouds: impacts on South Asian climate and hydrological cycle. *Proceedings of the National Academy of Sciences* **102**: 5326–5333, Doi 10.1073/pnas.0500656102.

Ramanathan V, Crutzen PJ, Lelieveld J, Mitra AP, Althausen D, Anderson J, Andreae MO, Cantrell W, Cass GR, Chung CE, Clarke AD, Coakley JA, Collins WD, Conant WC, Dulac F, Heintzenberg J, Heymsfield AJ, Holben B, Howell S, Hudson J, Jayaraman A, Kiehl JT, Krishnamurti TN, Lubin D, McFarquhar G, Novakov T, Ogren JA, Podgorny IA, Prather K, Priestley K, Prospero JM, Quinn PK, Rajeev K, Rasch P, Rupert S, Sadourny R, Satheesh SK, Shaw GE, Sheridan P, Valero FPJ. 2001a. Indian Ocean Experiment: an integrated analysis of the climate forcing and effects of the great Indo-Asian haze. *Journal of Geophysical Research* **106**: 28371–28398.

Roderick ML, Farquhar GD. 2002. The cause of decreased pan evaporation over the past 50 years. *Science* **298**: 1410–1411.

Rossow WB. 1989. Measuring cloud properties from space: a review. *Journal of Climate* **2**: 201–213.

Rossow WB, Laci AA. 1990. Global, seasonal cloud variations from satellite radiance measurements. Part II. Cloud properties

and radiative effects. *Journal of Climate* **3**: 1204–1253, DOI: 10.1175/1520-0442.

Rossow WB, Schiffer RA. 1991. ISCCP cloud data products. *Bulletin of the American Meteorological Society* **72**: 2–20.

Rossow WB, Walker AW, Garder LC. 1993. *Comparison of ISCCP and Other Cloud Amounts*. Journal of Climate **6**: 2394–2418.

Rossow WB, Schiffer RA. 1999. Advances in understanding clouds from ISCCP. *Bulletin of the American Meteorological Society* **80**: 2261–2288.

Stackhouse PW Jr, Gupta SK, Cox SJ, Chiacchio M, Mikovitz JC. 2001. *The WCRP/GEWEX Surface Radiation Budget Project Release 2: An Assessment of Surface Fluxes at 1 Degree Resolution*. National Aeronautics and Space Administration: Washington, DC.

Stanhill G, Cohen S. 2001. Global dimming: a review of the evidence for a widespread and significant reduction in global radiation with discussion of its probable causes and possible agricultural consequences. *Agricultural and Forest Meteorology* **107**: 255–278.

Supit I, van Kappel RR. 1998. A simple method to estimate global radiation. *Solar Energy* **63**: 147–160.

Tarasova TA, Nobre CA, Eck TF, Holben BN. 2000. Modeling of gaseous, aerosol, and cloudiness effects on surface solar irradiance measured in Brazil's Amazonia 1992–1995. *Journal of Geophysical Research* **105**: 26961–26970.

Warren SG, Eastman RM, Hahn CJ. A survey of changes in cloud cover and cloud types over land from surface observations, 1971–1996. *Journal of Climate* (in press).

Wielicki BA, Wong T, Allan RP, Slingo A, Kiehl JT, Soden BJ, Gordon CT, Miller AJ, Yang S-K, Randall DA. 2002. Evidence for large decadal variability in the tropical mean radiative energy budget. *Science* **295**: 841–844.